A&A 655, A23 (2021)
https://doi.org/10.1051/0004-6361/202141275
© ESO 2021

Astronomy & Astrophysics

Gaia-ESO survey: Lithium abundances in open cluster Red Clump stars⋆,⋆⋆

L. Magrini[1], R. Smiljanic[2], E. Franciosini[1], L. Pasquini[3], S. Randich[1], G. Casali[4,5], C. Viscasillas Vázquez[6], A. Bragaglia[7], L. Spina[8], K. Biazzo[9], G. Tautvaišienė[6], T. Masseron[10,11], M. Van der Swaelmen[1], E. Pancino[1,12], F. Jiménez-Esteban[13], G. Guiglion[14], S. Martell[15], T. Bensby[16], V. D'Orazi[8], M. Baratella[8,17], A. Korn[16], P. Jofre[18], G. Gilmore[19], C. Worley[19], A. Hourihane[19], A. Gonneau[19], G. G. Sacco[1], and L. Morbidelli[1]

(Affiliations can be found after the references)

Received 10 May 2021 / Accepted 26 August 2021

ABSTRACT

Context. It has recently been suggested that all giant stars with masses below 2 $M_\odot$ suffer an episode of surface lithium enrichment between the tip of the red giant branch (RGB) and the red clump (RC).
Aims. We test if the above result can be confirmed in a sample of RC and RGB stars that are members of open clusters.
Methods. We discuss Li abundances in six open clusters with ages between 1.5 and 4.9 Gyr (turn-off masses between 1.1 and 1.7 $M_\odot$). We compare these observations with the predictions of different models that include rotation-induced mixing, thermohaline instability, mixing induced by the first He flash, and energy losses by neutrino magnetic moment.
Results. In six clusters, we find close to 35% of RC stars have Li abundances that are similar or higher than those of upper RGB stars. This can be a sign of fresh Li production. Because of the extra-mixing episode connected to the luminosity bump, the expectation has been for RC stars to have systematically lower surface Li abundances. However, we cannot confirm that this possible Li production is ubiquitous. For about 65% of RC giants, we can only determine upper limits in abundances that could be hiding very low Li content.
Conclusions. Our results indicate the possibility that Li is being produced in the RC, at levels that would not typically permit the classification of these the stars as Li rich. The determination of their carbon isotopic ratio would help to confirm that the RC giants have suffered extra mixing followed by subsequent Li enrichment. The Li abundances of the RC stars can be qualitatively explained by the models including an additional mixing episode close to the He flash.

Key words. stars: abundances – stars: evolution – stars: low-mass – open clusters and associations: general

1. Introduction

The existence of lithium-rich giants has been known for many years (see, e.g. Brown et al. 1989; Charbonnel & Balachandran 2000; Monaco et al. 2011; Kumar et al. 2011). However, their nature continues to stand as a mystery that has not yet been fully resolved. Many studies have shown that they amount to ∼1−2% of all giant stars (see, e.g. Casey et al. 2016; Smiljanic et al. 2018; Deepak & Reddy 2019; Martell et al. 2021; Charbonnel et al. 2020). Recent results based on a combination of spectroscopic and asteroseismic observations have indicated the predominance of Li-rich giants in the core-helium-burning 'red clump' (RC) phase (Silva Aguirre et al. 2014; Casey et al. 2019; Kumar & Reddy 2020; Deepak & Lambert 2021; Yan et al. 2021; Singh et al. 2019, 2021). Kumar et al. (2020) performed a large-scale investigation of the Li content in field stars at the RC phase and claimed that most of them show high levels of surface Li abundance for their evolutionary stage, with A(Li)[1] > −0.9. Hence, these authors have suggested that a systematic production of Li in low-mass stars (i.e. those with mass below 2 $M_\odot$) is present between the tip of the red giant branch (RGB) and the RC. The Li abundance in cluster giants was originally discussed by Pasquini et al. (2001), who presumed that RC stars could have more Li than stars during the first ascent of the RGB. Subsequent observations of giant stars in the open cluster IC 4651 (Pasquini et al. 2004) supported this hypothesis, since they observed only upper limits for the stars that are found away from the RC, while they could measure the Li in the RC stars.

Here, we take advantage of the sixth internal data release of the *Gaia*-ESO Survey (IDR6, Gilmore et al. 2012; Randich et al. 2013) to explore the problem of Li abundances in RC stars from the point of view of open clusters. These objects give us the possibility to determine the ages and main-sequence turn-off (MSTO) masses with a high level of accuracy from isochrone fittings of their evolutionary sequence. The MSTO masses can be further used as proxy of the masses of the evolved stars. The comparison with isochrones also allows us to separate the RC stars from the RGB stars. We can thus study the evolution of the Li surface abundance along stellar evolutionary phases across different mass ranges.

⋆ Full Tables 2 and 3 are only available at the CDS via anonymous ftp to cdsarc.u-strasbg.fr (130.79.128.5) or via http://cdsarc.u-strasbg.fr/viz-bin/cat/J/A+A/655/A23

⋆⋆ Based on observations collected with the FLAMES instrument at VLT/UT2 telescope (Paranal Observatory, ESO, Chile), for the *Gaia*-ESO Large Public Spectroscopic Survey (188.B-3002, 193.B-0936, 197.B-1074).

[1] $A(Li) = \log(\frac{X(Li)}{X(H)} \cdot \frac{A_H}{A_{Li}}) + 12$, where X and A are the mass fraction and the atomic mass.

Table 1. Six open clusters with well populated giant branches.

Cluster	Age (Gyr)	D (kpc)	R_{GC} (kpc)	[Fe/H] (dex)	MSTO ($M_\odot$)	RC ($M_\odot$)
NGC 2158	1.5	4.3	12.6	-0.16 ± 0.05	1.7	1.8
NGC 2141	1.9	5.2	13.3	-0.06 ± 0.07	1.6	1.7
Berkeley 21	2.1	6.4	14.7	-0.21 ± 0.04	1.5	1.6
Trumpler 5	4.3	3.0	11.2	-0.35 ± 0.04	1.1	1.2
NGC 2243	4.4	3.7	10.6	-0.44 ± 0.09	1.1	1.2
Berkeley 32	4.9	3.1	11.1	-0.28 ± 0.08	1.1	1.2

Notes. Age, distance, and Galactocentric distance are from Cantat-Gaudin et al. (2020). Mean [Fe/H] are from the members observed with the UVES spectrograph in *Gaia*-ESO IDR6. MSTO and RC masses are obtained using PARSEC isochrones (Bressan et al. 2012).

2. Sample selection

For our analysis, we used a selection of member stars from the sample of 57 open clusters with stellar parameters from *Gaia*-ESO IDR6 and analyzed in Magrini et al. (2021, hereafter M21). We refer to that paper for a description of the *Gaia*-ESO analysis and the membership selection procedure.

We defined two different samples: the first is composed of all cluster members with $1\,M_\odot \leq M_{\rm MSTO} \leq 1.8\,M_\odot$ and a restricted range of metallicity, namely: $-0.2 \leq$ [Fe/H] $\leq +0.2$ dex, belonging to the clusters Col 261, Be 39, NGC 6791, M 67, Haf 10, Cz 24, NGC 2425, Trumpler 20, NGC 2141, NGC 2420, NGC 2158, NGC 2154; we use this sample for a first global comparison with the models. For the second sample, we select six open clusters with well-populated giant branches for a more detailed comparison with the models. These clusters have an age between 1550 and 4900 Myr, hosting at least ~20 red giant stars for which Li abundance is available, presenting a clearly distinguishable RC, and they are characterised by $1.1\,M_\odot \leq M_{\rm MSTO} \leq 1.7\,M_\odot$ (Table 1).

Lithium in the selected clusters was measured from UVES spectra for RC stars, and either from UVES (if available) or GIRAFFE data for the remaining members (see Fig. A.1 for two examples of spectra). When the line was too weak and barely visible (or not at all), upper limits were provided (see M21 for details). Lithium abundances in *Gaia*-ESO are derived using one-dimensional (1D) model atmospheres in local thermodynamical equilibrium (LTE). M21 estimated that the abundance corrections based on more realistic 3D non-LTE model atmospheres (Wang et al. 2021) are within ±0.1 dex, depending on $T_{\rm eff}$, and almost negligible for MSTO stars and for giant stars hotter than 4200 K. We thus adopted the 1D LTE *Gaia*-ESO Li abundances.

3. Li abundance in RC stars

Recently, Kumar et al. (2020) investigated Li abundances in field RC stars with masses below $2.0\,M_\odot$, using the results of the GALactic Archaeology with HERMES (GALAH) survey (DR2, Buder et al. 2018). They found the RC stars to have enhanced Li when compared to stars at the RGB tip, and with respect to a $1.0\,M_\odot$ model that includes effects of extra mixing (thermohaline instability and rotation-induced mixing). This led to the suggestion that Li production is a general phenomenon that affects all low-mass stars between the RGB tip and the RC.

To test the above hypothesis, we identify RC stars in our first sample of cluster members by comparing their location in the Hertzprung-Russel diagrams with isochrones. We chose the RC stars in our sample as those with $4600 \leq T_{\rm eff}\,({\rm K}) \leq 5000$ and $1.5 \leq \log(L/L_\odot) \leq 1.9$ (see Fig. 1). With this selection, there might still be some contamination from RGB stars, but the probability is low. A star with a mass between 1 and $1.8\,M_\odot$, during the RGB phase, spends approximately $0.2{-}0.4 \times 10^8$ yr with the same luminosity of a RC star, while it stays in the RC phase 2−5 times longer (see also Singh et al. 2021 for an estimate of the timescales of the RC phase). In addition, the difference in $T_{\rm eff}$ between the two phases at the luminosity of giant stars varies from ~300 K at $1\,M_\odot$ to ~150 K at $1.8\,M_\odot$, which is considerably larger than our typical errors (30−60 K) and allows us to separate the two phases. In our sample, we have 53 RC stars with A(Li) measurements and 50 with upper limits. The identifying names based on the equatorial coordinates, called CNAMEs, cluster to which they belong, stellar parameters, lithium abundances, and MSTO masses of the selected RC stars are reported in Table 2.

In Fig. 1, we plot the stars in the A(Li)–$\log(L/L_\odot)$ plane. Two sets of models at solar metallicity for 1.5 and $2\,M_\odot$ stars from Lagarde et al. (2012) are shown. One set includes only effects of mixing due to convection. In addition, the second includes rotation-induced mixing and thermohaline instability (hereafter, the RT models). The figure shows the evolution of the lithium abundances: on the left, we have stars at the end of the main sequence, where A(Li) is between 2.5 and 3.4 dex. Afterwards, there is a first episode of dilution at the first dredge-up (FDU) which, in classical models, gives a value of $A({\rm Li}) \sim 1.3{-}1.5$, almost independent of stellar mass. In the RT models, the FDU results in lower Li because of the effects of rotation during the main sequence. In addition, there is a further dilution of Li at the RGB bump when the thermohaline instability is activated. After that, stars evolve towards the RGB tip and then drop in luminosity, reaching the RC at $\log(L/L_\odot) \sim 1.5{-}1.8$. The models suggest Li abundances as low as −0.3 dex in the RGB phase. Further evolution during the clump can deplete Li down to −1 dex before the stellar luminosity increases again.

The RC stars in our sample with $1\,M_\odot \leq M < 1.8\,M_\odot$ have $-0.9 \leq A({\rm Li}) \leq 1.3$. This is higher than predicted by RT models but lower than predicted by classical models (excluding the two Li-rich giants). The mean A(Li) of the RC stars is $A({\rm Li}) = 0.78 \pm 0.55$ dex (only measurements, no upper limits). This value is close to the peak of the distribution obtained by Kumar et al. (2020), $A({\rm Li}) \sim 0.7$ dex. These data are thus consistent with their findings and suggest that there might be a further Li enrichment during the RC phase.

Figure 2 shows, separately, the six clusters of Table 1 in the $\log(L/L_\odot)$ versus the A(Li) plane and in the HR diagram. Properties such as their CNAMEs, cluster to which they belong, stellar parameters, lithium abundances, MSTO mass, and the evolutionary phase of the selected RGB and RC stars are reported in Table 3.

As discussed in M21, for low-mass solar-type stars with relatively extended convective envelopes, hydrodynamic processes induced by rotation, such as meridional circulation and shear mixing, predict large rotation gradients within the interior, which, for instance, require internal gravity waves or other mechanisms, such as penetrative convection, tachocline mixing, and additional turbulence to explain the rotation profile and the surface abundance of lithium in solar-type stars of various ages. These additional mechanisms are not included in the RT models of Lagarde et al. (2012) for $1\,M_\odot$ stars. Since in RT models for $1\,M_\odot$ stars at solar metallicity, the depletion of Li in the RGB phase reaches extremely low values not corresponding to the observed abundances, we consider more suitable to compare

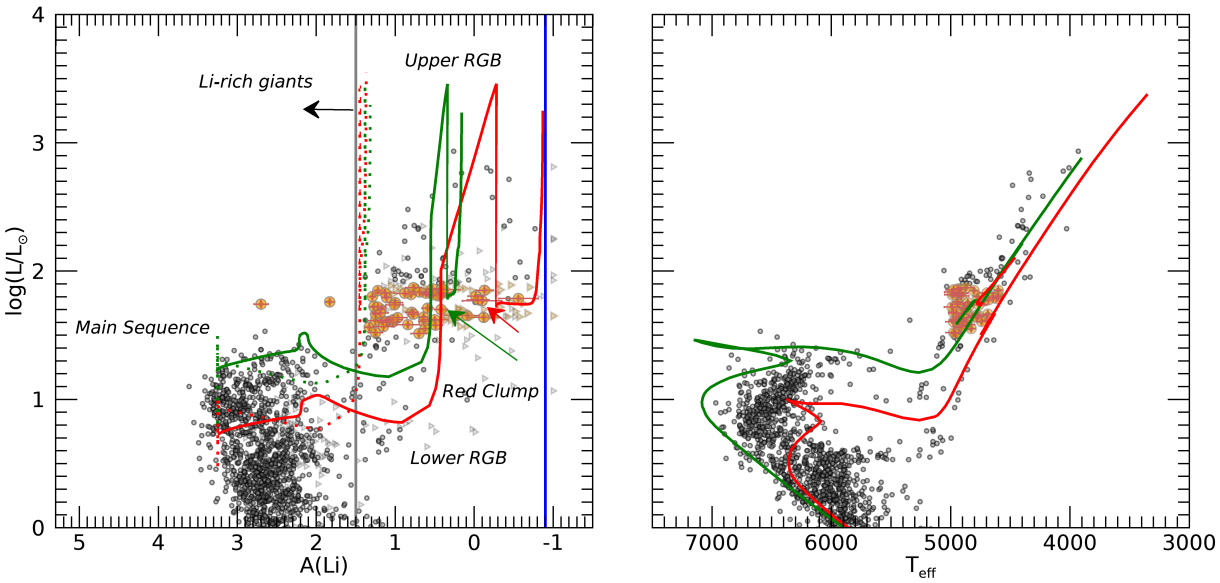

Fig. 1. Lithium abundance and stellar parameters of member stars of open clusters with $1\,M_{\odot} \leq M \leq 1.8\,M_{\odot}$ and $-0.2 \leq$ [Fe/H] ≤ 0.2. *Left panel*: $\log(L/L_{\odot})$ versus A(Li); grey circles show the whole sample of member stars and coloured circles the stars at the RC. Triangles show the upper limits on A(Li). The red and green continuous curves are the RT models at solar metallicity for $1.5\,M_{\odot}$ and $2\,M_{\odot}$, respectively, while the red and green dotted curves are the classical models for the same masses from Lagarde et al. (2012). The vertical black line indicates the limit for Li-rich giants $A(\mathrm{Li}) \geq 1.5$ dex, while the vertical blue line at $A(\mathrm{Li}) \geq -0.9$ dex shows the RC-RGB limit of Kumar et al. (2020). The locations of the RC in the RT models of Lagarde et al. (2012) are shown with arrows. *Right panel*: HR diagram with the sample stars and the PARSEC isochrones for 1.5 and $2.0\,M_{\odot}$, in red and green, respectively, at solar metallicity.

Table 2. Red clump member stars of open clusters with $1\,M_{\odot} \leq M_{\mathrm{MSTO}} \leq 1.8\,M_{\odot}$ and $-0.2 \leq$ [Fe/H] ≤ 0.2.

CNAME	Cluster	T_{eff} (K)	log g	[Fe/H]	A(Li)	UL$_{A(\mathrm{Li})}$ [a]	log $(L/L_{\odot})$	MSTO $(M_{\odot})$
07465009–0436004	Berkeley 39	4820 ± 30	2.62 ± 0.05	-0.14 ± 0.17	0.64 ± 0.05	0	1.64 ± 0.03	1.2
07470378–0439141	Berkeley 39	4700 ± 30	2.52 ± 0.05	-0.14 ± 0.05	1.17 ± 0.06	0	1.62 ± 0.03	1.2

Notes. The full table is available online at the CDS. [a]Upper limits are indicated with 1, detections with 0.

the observations of all our sample clusters with the models for $1.5\,M_{\odot}$.

The stars are divided in lower RGB (if below the luminosity bump when compared to an isochrone), upper RGB (if above the bump), and RC. It is clear that the distributions of Li abundances in the RC stars of each cluster show values that are either similar or even higher than those of the upper RGB stars. In standard models, the Li abundance reaches ∼1.5 dex after the first dredge-up, with no further changes up to the RC. Traditionally, only giants with $A(\mathrm{Li}) > 1.5$ are considered to be Li-rich. In the RT model, rotation-induced mixing brings A(Li) down to ∼0.4 after the first dredge-up and thermohaline mixing reduces it to ∼−0.3 dex after the bump. Figure 2 shows that each evolutionary stage in each cluster is characterised by a spread in Li abundances. This can be explained by a spread in the initial stellar rotation and thus in the effects of the rotation-induced mixing (e.g. Charbonnel et al. 2020). In other words, the fact that a given star, at any evolutionary stage, has an observed Li abundance above the model prediction does not immediately imply that Li was produced. Observed values above the model prediction can be explained by a weaker action on the part of rotation-induced mixing since initial rotation is a property that is known to vary considerably from star to star (e.g. Gallet & Bouvier 2013).

To determine whether or not there is Li production in the RC, it is necessary to investigate the general properties of the abundance distributions in each evolutionary stage. The differences in the distribution of Li abundances between lower RGB and RC stars indicates a certain level of Li depletion by thermohaline mixing. The brighter RGB stars in NGC 2158 and NGC 2141 show signs of extra Li depletion after the bump. It seems fair to assume that the depletion will increase before the stars reach the RGB tip and the RC. Therefore, it does indeed seem that fresh Li production is needed in order to explain how the RC stars can have similar or higher Li than the upper RGB stars.

This finding is in agreement with the conclusions of Kumar et al. (2020). However, we remark that about 65% of our RC stars have Li upper limits; some at the same level of the detected abundances. The remaining 35% RC stars have Li measurements at the level of the lower RGB abundances and higher than the upper RGB ones. Thus, strong Li depletion in some of the giants cannot be excluded. Either the Li-rich stage is short-lived (see Singh et al. 2021) or Li production is not ubiquitous. In the GALAH data used by Kumar et al. (2020), upper limits are not flagged. If some of the Li abundances these authors discuss are actually the upper limits, then perhaps not all of their RC stars have high Li abundance.

4. Possible mechanisms to explain Li in RC stars

4.1. Mixing induced by the first He flash

Motivated by the Li discrepancy highlighted by Kumar et al. (2020) between tip-RGB and RC stars, Schwab (2020) recently proposed a model where the He flash is connected to the

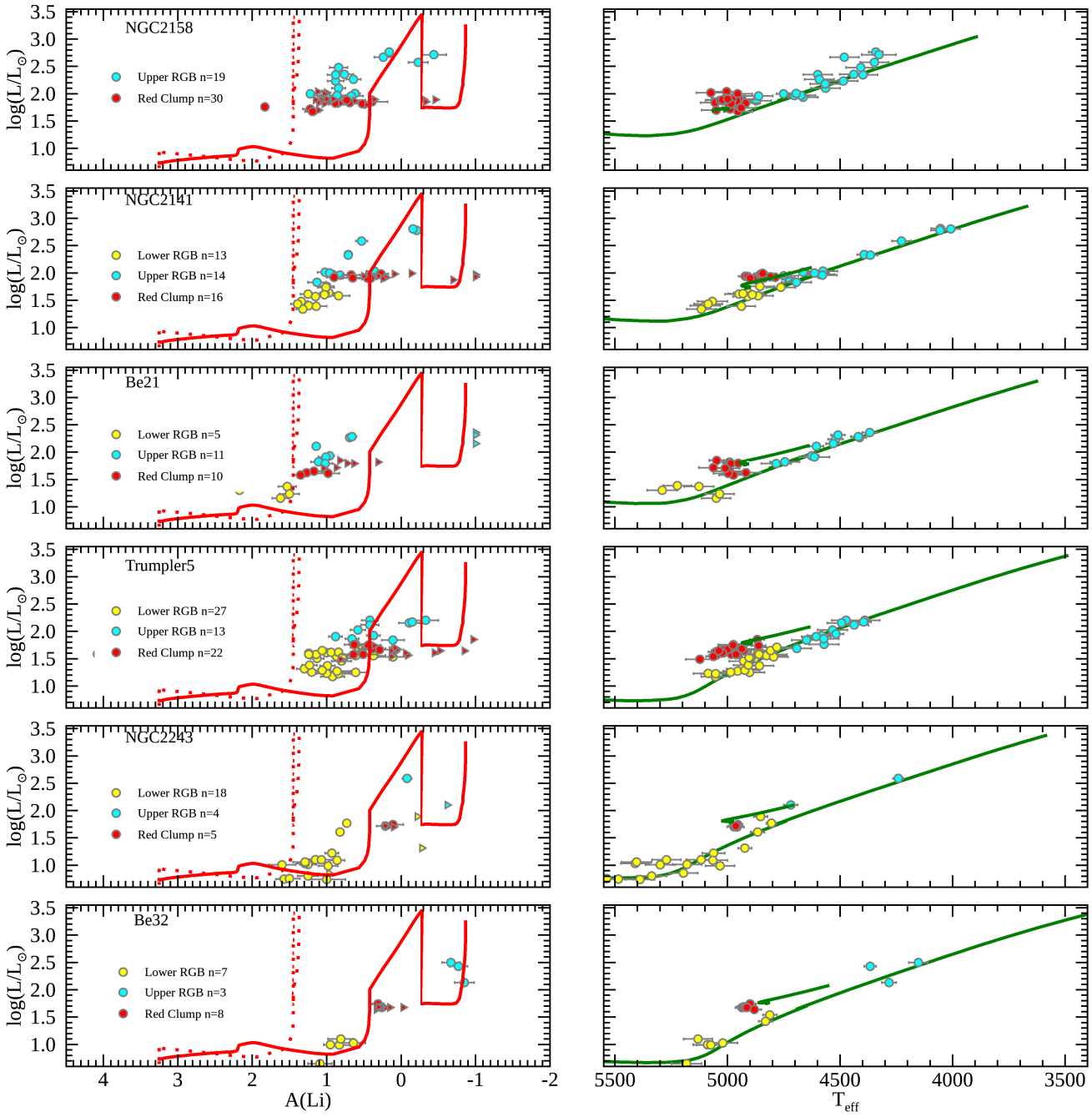

Fig. 2. Lithium abundance and stellar parameters of member stars in our sample clusters. *Left panels*: $\log(L/L_{\odot})$ versus A(Li); yellow circles are lower RGB stars – prior to the RGB bump –, cyan circles are upper RGB stars – after the bump – and red circles are RC stars. The red continuous curves are the models with rotation-induced mixing at solar metallicity for 1.5 $M_{\odot}$. The red dotted curves are the classical models with only convection from Lagarde et al. (2012). *Right panels*: HR diagrams with the PARSEC isochrones (Bressan et al. 2012) at the age and metallicity of each cluster. The error bars on luminosity are of the order of the symbol size.

surface Li enhancement. The model of Schwab (2020) is constructed using Modules for Experiments in Stellar Astrophysics (MESA, see e.g. Paxton et al. 2019). Thermohaline instability is included, but rotation-induced mixing is not taken into account, as this approach is different from that of the RT models. Lithium production is a result of the Cameron-Fowler (CF) process (Cameron & Fowler 1971), resulting from the decay of ^{7}Be produced in internal regions with temperatures above $\sim 10^{7}$ K. In their model, the mixing in the envelope is triggered by the first and strongest He sub-flash. The physical mechanism that induces this mixing might be due to internal gravity waves (see Schwab 2020 for a discussion).

In Fig. 3, we compare A(Li) in our sample of six clusters with the results of models with and without the flash-induced mixing from Schwab (2020)[2]. The effect of thermohaline-induced mixing and of the flash-induced mixing both depend on mass and are stronger for lower masses. For the three younger clusters (NGC 2158, NGC 2141, and Be 21), the models without the

[2] https://doi.org/10.5281/zenodo.4688026

Table 3. RGB and RC member stars of the six open clusters of Table 1.

CNAME	Cluster	$T_{\rm eff}$ (K)	log g	[Fe/H]	A(Li)	UL$_{\rm A(Li)}$ [(a)]	log ($L/L_\odot$)	MSTO ($M_\odot$)	Phase
05513791+2143345	Berkeley 21	5223 ± 64	3.63 ± 0.18	−0.34 ± 0.06	0.83	1	1.39 ± 0.03	1.5	LRGB
05515065+2148321	Berkeley 21	5127 ± 66	3.21 ± 0.18	−0.07 ± 0.05	1.53 ± 0.12	0	1.37 ± 0.03	1.5	LRGB

Notes. The full table is available online at the CDS. [(a)]Upper limits are indicated with 1, detections with 0.

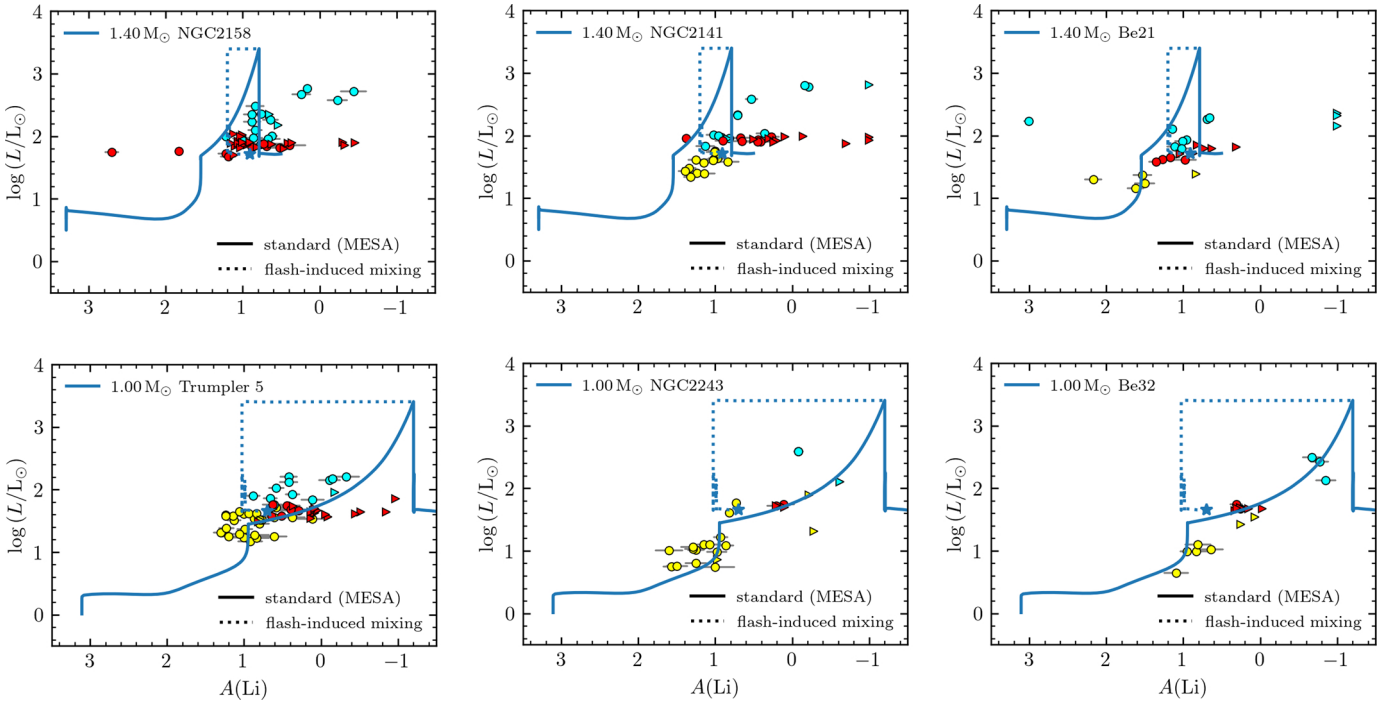

Fig. 3. Luminosity versus A(Li) in NGC 2158, NGC 2141, Be 21, Trumpler 5, NGC 2243, and Be 32. Symbols are the same as in Fig. 2. The blue continuous curves are the MESA models with thermohaline mixing. The blue dotted curves are the models with flash-induced mixing of Schwab (2020). The stellar mass of the models is indicated in each panel.

flash-induced mixing for 1.4 $M_\odot$ can reproduce quite well the A(Li) in the RC stars. The extra mixing during the He flash is not totally necessary to explain A(Li) in the RC. The results are similar to those obtained with the RT models presented in Fig. 2. We note, however, that upper RGB stars have lower A(Li) than predicted by the models of Schwab (2020); this is probably because the effect of rotation is not included. However, our aim is to make a qualitative comparison and introducing the effect of rotation goes beyond what we set out to do in this paper. For the oldest clusters (Trumpler 5, NGC 2243, Be 32), A(Li) in RC stars is definitively higher than the prediction of models without flash-induced mixing. The agreement is better with models that include the new extra-mixing after the tip of the RGB. Nevertheless, our data seem to indicate a slightly lower efficiency of the diffusive mixing process than the one adopted in Schwab (2020).

4.2. Mixing induced by neutrino magnetic moment

To explain the ubiquitous enhancement of Li in RC stars, Mori et al. (2021) introduced an additional energy loss related to the neutrino magnetic moment (NMM), μ_ν (see also Mori et al. 2020). These authors used the MESA code to build a fiducial model with $\mu_\nu = 0$ and a set of models with μ_{12} ranging from 1 to 5, where $\mu_{12} = \mu_\nu/10^{-12}\mu_{\rm B}$ and $\mu_{\rm B}$ is the Bohr magneton. Assuming $\mu_\nu > 0$, the He flash is delayed and the CF mechanism can continue to produce Li. The delayed He flash results in stars with heavier He core and increased luminosity at the RGB tip. More massive cores have a smaller density above the hydrogen burning shell and, consequently, a larger thermal conductivity (Lattanzio et al. 2015) and a more effective thermohaline mixing. The enhanced mixing increases the amount of ^{7}Be transported to the surface convective layer, resulting in higher Li in RC stars.

In Fig. 4, we compare our observations with the Mori et al. (2021) models. The effect of NMM for the younger clusters is limited, and there are negligible differences with respect to the standard models. As in the models of Schwab (2020), the standard model is not able to reproduce the depletion observed towards the RGB tip. For the three older clusters, the standard models would predict lower A(Li) in the RC stars, while models with higher μ_{12} cover quite well the observed range of A(Li). However the highest values of NNM are slightly higher than current astrophysical limits for this quantity; thus, also other channels may play a role in explaining the behaviour of RC stars.

Both the models of Schwab (2020) and Mori et al. (2021) appear to be equipped to explain the observations of A(Li) in low-mass RC stars ($M \sim 1\,M_\odot$). The two scenarios, however, differ in the timescales of the processes, as described in Mori et al. (2021). In the He-flash mixing model, A(Li) is enhanced during the helium flash. In the NMM model, the enhancement happens on a longer time scale, namely, about 1 Myr before the flash. As suggested by Mori et al. (2021), it

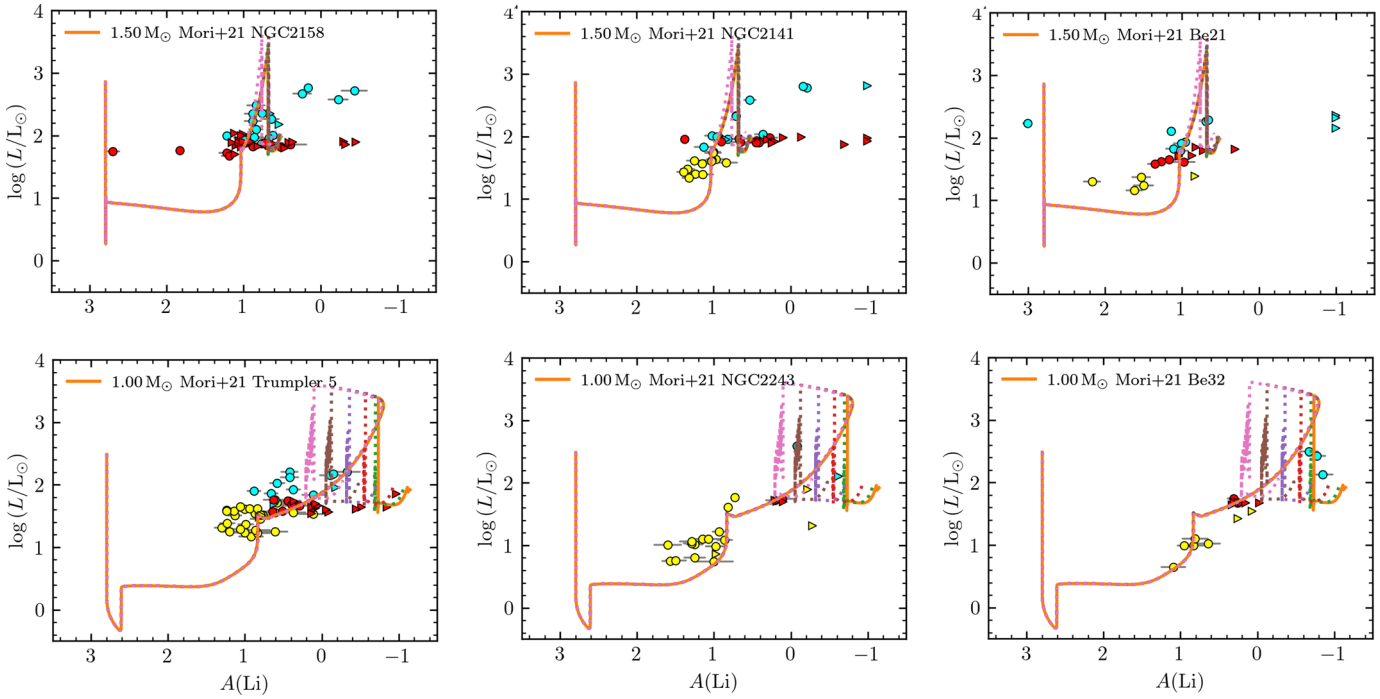

Fig. 4. Comparison of $\log(L/L_\odot)$ versus A(Li) in NGC 2158, NGC 2141, Be 21, Trumpler 5, NGC 2243, and Be 32: symbols and colours are the same as for the observations as in Fig. 3. The orange continuous curves are the MESA models with thermohaline mixing for the masses indicated in each panel, and $\mu_{12} = 0$. The dotted curves are the models with NMM mixing of Mori et al. (2021) for 1 $M_\odot$ and different μ_{12}, from 1 to 5, from right to left.

might be possible to distinguish between the two models by searching for lithium-rich giant stars with $A(\mathrm{Li}) \sim 0$ near the tip of the RGB.

We briefly remark that Masseron et al. (2017) identified significant N depletion in field stars between the RGB tip and the RC, supporting the need for extra mixing between these phases. In this case, nitrogen has to be burnt near or at the He flash episode before the material is mixed to the surface.

5. Summary and conclusions

Here, we investigate the evolution of A(Li) from the MSTO to the RGB and RC phases using a sample of red giants in open clusters from *Gaia*-ESO IDR6. We find RC stars where Li is detected at a level consistent with or above those of upper RGB stars. This suggests that there might be some Li enrichment between these phases that results in stars that would typically not be classified as Li-rich. Going forward, it would be useful to determine the carbon isotopic ratio in these RC stars and to confirm that they have gone through the extra mixing after the luminosity bump.

Nevertheless, our sample has several RC giants with Li upper limits, across the whole mass range. These limits are, for about 65% of our RC stars in individual clusters, at the same level of the detected Li abundances (the lines are always very weak and hard to detect; see Appendix A). Upper limits could be hiding strong Li depletion in these stars. It appears that upper limits are not properly flagged in the data used by Kumar et al. (2020). Therefore, their sample might also include RC stars with strong Li depletion. However, for 35% of our RC stars in the clusters of Table 1, the Li abundance is at the level of that in lower RGB stars, and usually higher than in upper RGB stars. Given these percentages, we cannot conclude that Li enrichment is ubiquitous in RC stars, as their Li abundances could be much lower, but that it might happen in a large percentage of them: from at least one third up to one half of them (see the sample in Fig. 1).

The comparison with models that include additional mixing processes, for instance, the He-flash mixing (Schwab 2020) and the NMM mixing (Mori et al. 2021), is very promising and has the capacity to qualitatively explain the behaviour of the RC stars. Both models work quite well to explain the behaviour of low-mass stars ($M \sim 1\,M_\odot$). While they differ in terms of the description of the processes that activate the CF mechanisms and their timescales, they do agree on the requirement of a process of mixing during the He flash that is needed to activate the production of Li.

Acknowledgements. We thank an anonymous referee for her/his careful reading of the manuscript and for useful and constructive comments. We thank J. Schwab for recomputing for us his models (available at https://doi.org/10.5281/zenodo.4688026), and for useful discussion and comments. We thank K. Mori for kindly providing us his models to compare with our data. Based on data products from observations made with ESO Telescopes at the La Silla Paranal Observatory under programme ID 188.B-3002. These data products have been processed by the Cambridge Astronomy Survey Unit (CASU) at the Institute of Astronomy, University of Cambridge, and by the FLAMES/UVES reduction team at INAF/Osservatorio Astrofisico di Arcetri. These data have been obtained from the *Gaia*-ESO Survey Data Archive, prepared and hosted by the Wide Field Astronomy Unit, Institute for Astronomy, University of Edinburgh, which is funded by the UK Science and Technology Facilities Council. This work was partly supported by the European Union FP7 programme through ERC grant number 320360 and by the Leverhulme Trust through grant RPG-2012-541. We acknowledge the support from INAF and 'Ministero dell'Istruzione, dell'Università' e della Ricerca (MIUR) in the form of the grant "Premiale VLT 2012". The results presented here benefit from discussions held during the *Gaia*-ESO workshops and conferences supported by the ESF (European Science Foundation) through the GREAT Research Network Programme. LM, GC, AB, MVdS, EP acknowledge the funding from MIUR Premiale 2016: MITiC. MVdS and LM thanks the WEAVE-Italia consortium. LM acknowledges the funding from the INAF PRIN-SKA 2017 program 1.05.01.88.04. CVV, LM, EP thank

the COST Action CA18104: MW-*Gaia*. LS acknowledges financial support from the Australian Research Council (discovery Project 170100521) and from the Australian Research Council Centre of Excellence for All Sky Astrophysics in 3 Dimensions (ASTRO 3D), through project number CE170100013. F.J.E. acknowledges financial support from the Spanish MINECO/FEDER through the grant AYA2017-84089 and MDM-2017-0737 at Centro de Astrobiología (CSIC-INTA), Unidad de Excelencia María de Maeztu, and from the European Union's Horizon 2020 research and innovation programme under Grant Agreement no. 824064 through the ESCAPE – The European Science Cluster of Astronomy & Particle Physics ESFRI Research Infrastructures project. TB was funded by grant No. 2018-04857 from The Swedish Research Council.

References

Bressan, A., Marigo, P., Girardi, L., et al. 2012, MNRAS, 427, 127
Brown, J. A., Sneden, C., Lambert, D. L., & Dutchover, E., Jr. 1989, ApJS, 71, 293
Buder, S., Asplund, M., Duong, L., et al. 2018, MNRAS, 478, 4513
Cameron, A. G. W., & Fowler, W. A. 1971, ApJ, 164, 111
Cantat-Gaudin, T., Anders, F., Castro-Ginard, A., et al. 2020, A&A, 640, A1
Casey, A. R., Ruchti, G., Masseron, T., et al. 2016, MNRAS, 461, 3336
Casey, A. R., Ho, A. Y. Q., Ness, M., et al. 2019, ApJ, 880, 125
Charbonnel, C., & Balachandran, S. C. 2000, A&A, 359, 563
Charbonnel, C., Lagarde, N., Jasniewicz, G., et al. 2020, A&A, 633, A34
Deepak & Lambert, D. L. 2021, MNRAS, 505, 642
Deepak & Reddy, B. E. 2019, MNRAS, 484, 2000
Gallet, F., & Bouvier, J. 2013, A&A, 556, A36
Gilmore, G., Randich, S., Asplund, M., et al. 2012, The Messenger, 147, 25
Kumar, Y. B., & Reddy, B. E. 2020, JApA, 41, 49
Kumar, Y. B., Reddy, B. E., & Lambert, D. L. 2011, ApJ, 730, L12
Kumar, Y. B., Reddy, B. E., Campbell, S. W., et al. 2020, Nat. Astron., 4, 1059
Lagarde, N., Decressin, T., Charbonnel, C., et al. 2012, A&A, 543, A108
Lattanzio, J. C., Siess, L., Church, R. P., et al. 2015, MNRAS, 446, 2673
Magrini, L., Lagarde, N., Charbonnel, C., et al. 2021, A&A, 651, A84
Martell, S., Simpson, J., Balasubramaniam, A., et al. 2021, MNRAS, 505, 5340
Masseron, T., Lagarde, N., Miglio, A., Elsworth, Y., & Gilmore, G. 2017, MNRAS, 464, 3021
Monaco, L., Villanova, S., Moni Bidin, C., et al. 2011, A&A, 529, A90
Mori, K., Balantekin, A. B., Kajino, T., & Famiano, M. A. 2020, ApJ, 901, 115
Mori, K., Kusakabe, M., Balantekin, A. B., Kajino, T., & Famiano, M. A. 2021, MNRAS, 503, 2746
Pasquini, L., Randich, S., & Pallavicini, R. 2001, A&A, 374, 1017
Pasquini, L., Randich, S., Zoccali, M., et al. 2004, A&A, 424, 951
Paxton, B., Smolec, R., Schwab, J., et al. 2019, ApJS, 243, 10
Randich, S., Gilmore, G., & Gaia-ESO Consortium 2013, The Messenger, 154, 47
Schwab, J. 2020, ApJ, 901, L18
Silva Aguirre, V., Ruchti, G. R., Hekker, S., et al. 2014, ApJ, 784, L16
Singh, R., Reddy, B. E., & Kumar, Y. B. 2019, MNRAS, 482, 3822
Singh, R., Reddy, B. E., Campbell, S. W., Kumar, Y. B., & Vrard, M. 2021, ApJ, 913, L4
Smiljanic, R., Franciosini, E., Bragaglia, A., et al. 2018, A&A, 617, A4
Wang, E. X., Nordlander, T., Asplund, M., et al. 2021, MNRAS, 500, 2159
Yan, H.-L., Zhou, Y.-T., Zhang, X., et al. 2021, Nat. Astron., 5, 86

[1] INAF – Osservatorio Astrofisico di Arcetri, Largo E. Fermi 5, 50125 Firenze, Italy
e-mail: laura.magrini@inaf.it
[2] Nicolaus Copernicus Astronomical Center, Polish Academy of Sciences, ul. Bartycka 18, 00-716 Warsaw, Poland
[3] ESO, Karl Schwarzschild Strasse 2, 85748 Garching, Germany
[4] Dipartimento di Fisica e Astronomia, Università degli Studi di Bologna, Via Gobetti 93/2, 40129 Bologna, Italy
[5] INAF – Astrophysics and Space Science Observatory Bologna, Via Gobetti 93/3, 40129 Bologna, Italy
[6] Institute of Theoretical Physics and Astronomy, Vilnius University, Sauletekio Av. 3, 10257 Vilnius, Lithuania
[7] INAF – Osservatorio di Astrofisica e Scienza dello Spazio di Bologna, Via Gobetti 93/3, 40129 Bologna, Italy
[8] INAF – Padova Observatory, Vicolo dell'Osservatorio 5, 35122 Padova, Italy
[9] INAF – Rome Observatory, Via Frascati, 33, Monte Porzio Catone, RM, Italy
[10] Instituto de Astrofísica de Canarias, 38205 La Laguna, Tenerife, Spain
[11] Universidad de La Laguna, Dept. Astrofísica, 38206 La Laguna, Tenerife, Spain
[12] Space Science Data Center – Agenzia Spaziale Italiana, Via del Politecnico, s.n.c., 00133 Roma, Italy
[13] Departamento de Astrofísica, Centro de Astrobiología (CSIC-INTA), ESAC Campus, Camino Bajo del Castillo s/n, 28692 Villanueva de la Cañada, Madrid, Spain
[14] Leibniz-Institut für Astrophysik Potsdam (AIP), An der Sternwarte 16, 14482 Potsdam, Germany
[15] School of Physics, University of New South Wales, Sydney, NSW 2052, Australia
[16] Lund Observatory, Department of Astronomy and Theoretical Physics, Box 43, 221 00 Lund, Sweden
[17] Dipartimento di Fisica e Astronomia Galileo Galilei, Vicolo Osservatorio 3, 35122 Padova, Italy
[18] Núcleo de Astronomía, Facultad de Ingeniería y Ciencias, Universidad Diego Portales, Ejército 441, Santiago, Chile
[19] Institute of Astronomy, University of Cambridge, Madingley Road, Cambridge CB3 0HA, UK

Appendix A: Detection of weak Li lines

In Fig. A.1, we show two examples of the Li lines in a red clump star and in an upper RGB one observed with the UVES spectrograph. The observed spectra are compared with two sets of synthetic spectra, computed for the corresponding set of stellar parameters, but with different Li abundances: the measured one and A(Li) = −1.0. Although the observed Li lines are very weak, the figure clearly shows that a non-negligible amount of Li is present in the RC star, while the RGB one is compatible with A(Li) = −1.0.

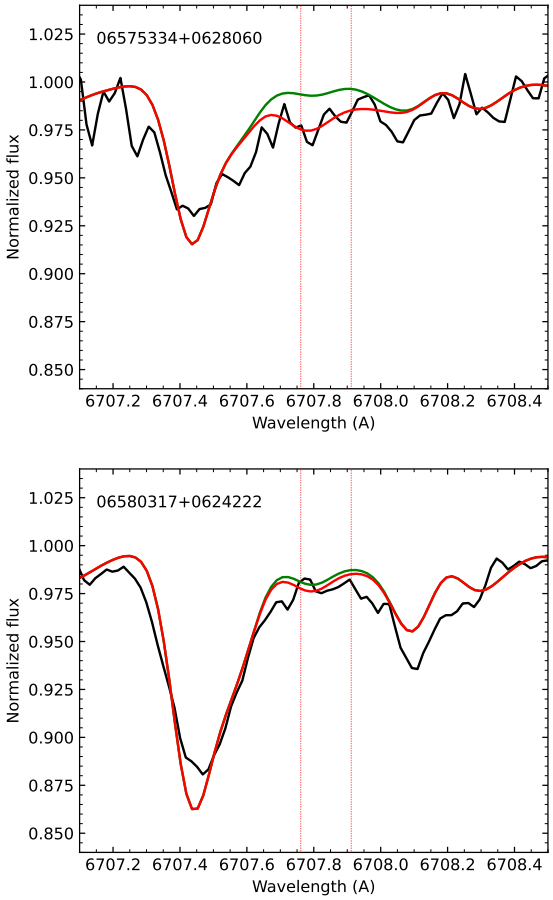

Fig. A.1. Spectral region around the Li doublet for an RC star (upper panel) and an upper RGB star (lower panel), both members of Berkeley 32. The observed spectra are in black. The red lines show the synthetic spectra at the corresponding measured stellar parameters and A(Li) (+0.3 and −0.8 dex, respectively); the green lines show the synthetic spectra for the same parameters and A(Li) = −1.0. The vertical lines indicate the location of the two Li lines.